Macromolecules
ARTICLE

Macromolecules **2009**, *42*, 7537–7544 **7537**
DOI: 10.1021/ma9006686

Modeling Microscopic Morphology and Mechanical Properties of Block Copolymer/Nanoparticle Composites

Jiezhu Jin[†] **and Jianzhong Wu***

Department of Chemical and Environmental Engineering, University of California, Riverside, California 92521

Amalie L. Frischknecht

Computational Materials Science and Engineering, Sandia National Laboratories, P.O. Box 5800 MS-1411, Albuquerque, New Mexico 87185-1411. [†]*Current address: Department of Materials Science and Engineering, The Pennsylvania State University, University Park, PA 16802*

Received March 27, 2009; Revised Manuscript Received June 24, 2009

ABSTRACT: The morphology of block copolymer and nanoparticle composites depends not only on the copolymer architecture but also on the surface energy, geometry, and volume fraction of the embedding nanoparticles. Toward a quantitative description of the composite structure and associated thermomechanical properties from a molecular perspective, we examined the performance of a nonlocal density functional theory that accounts for the excluded-volume effects and intra- and inter-chain correlations self-consistently. It is predicted that, within the lamellar structures of symmetric block copolymers, neutral particles are localized at the microdomain interface, leading to a reduction of the lamellar thickness. Conversely, particles that are energetically biased to a particular microdomain expand the block copolymer lamellar structure. The dilation or shrinkage of the lamellar thickness also depends on the particle packing density. Both particle dispersion and particle-polymer interfacial structure are highly sensitive to the ratio of the particle diameter to the lamellar thickness. While small nanoparticles may either increase or reduce the extensional moduli of the composite material depending on the nanoparticle volume fraction and polymer−particle interactions, large particles always enhance the mechanical properties regardless of the polymer−particle interactions. The theoretical predictions are found to be in qualitative agreement with simulation results and experiments.

1. Introduction

Polymer nanocomposites have been extensively investigated in recent years for potential applications in novel optoelectronic devices and high performance materials. Addition of nanoparticles to a polymer matrix introduces not only novel functionality but also improvements of the thermophysical properties, such as mechanical strength and thermal conductivity. Because the performance of a polymer nanocomposite is sensitive to the dispersion and arrangement of particles within the polymer matrix, it is important to control the morphology or microstructure of the polymer/particle mixtures during their synthesis. Toward that end, block copolymers are found to be particularly useful. The diverse ordered structures of block copolymers make them ideal as templates for controlling nanoparticle organization at nanometer scales.[1−3] By blending diblock copolymers with nanoparticles, one can create composites that integrate the polymer flexibility with novel optical, electromagnetic and mechanical properties of the particles.[3] Recent experiments demonstrated that distribution of nanoparticles in the microphase-separated morphologies of block copolymers leads to hierarchically structured composites that exhibit unusual optical or electrical properties.[4] Polymer nanocomposites with hierarchical structure may achieve unprecedented improvements in material stiffness, strength, and heat resistance, without compromising the flexibility and elasticity of the polymer matrix.[5]

*Corresponding author. E-mail: jwu@engr.ucr.edu.

The properties of a polymer−particle composite depend on a number of parameters, such as the particle size and volume fraction, the particle−polymer interaction energies, and polymer chain length and composition. These parameters are intimately related to the properties and performance of materials. Understanding the mechanism leading to modifications in the properties of nanocomposites is essential for design and application of copolymer nanocomposites with desired properties. For systems containing diblock polymers and nanoparticles, recent experiments and theoretical studies indicate that block copolymers are able to form a lamellar structure that guides the dispersion of nanoparticles in an energetically preferred microdomain or localized at the lamellar interface, depending on the particle-polymer surface energy.[1,4,6,7] While the distribution of nanoparticles can often be intuitively understood in terms of energy and entropy arguments, a quantitative description of the composite structure and phase behavior requires a molecular theory that accounts for all parameters pertinent to both block copolymers and the nanoparticles.

Addition of nanoparticles into a polymer matrix results in changes of the mechanical properties that are of interest from fundamental perspective and of technological importance. Efforts have been made to understand the elastic properties of diblock copolymers in the lamellar phase by using various theoretical methods. An important step in this direction was taken by Tyler and Morse,[8] who used a method proposed by Kossuth et al.[9] to obtain the linear elastic properties of the cubic phases of a diblock copolymer. They studied the gyroid and

Published on Web 09/08/2009

body-centered-cubic phases of diblock copolymers by using a theory of polymer elasticity and the polymer self-consistent-field theory (SCFT). Thompson et al.[10] examined the elastic properties of nanosphere-filled block copolymer nanocomposites using a hybrid SCFT and predicted that introduction of nanospheres into the lamellar phase of a diblock copolymer results in a lower tensile modulus in comparison to that of a pure diblock copolymer.

Polymer density functional theory (DFT) provides an effective mathematical framework to bridge phenomenological methods with time-consuming molecular simulations. On the one hand, DFT is able to retain the microscopic details of a macroscopic system at a computational cost significantly lower than that used in Monte Carlo/molecular dynamics simulations. The numerical efficiency makes DFT more convenient for practical applications that often require careful calibration of the molecular models. It yields structural and thermodynamic properties directly from the free-energy functional instead of indirect simulation of mechanical variables. On the other hand, DFT is theoretically more rigorous than phenomenological methods; it provides a unifying framework for various phenomenological methods that are originally developed in very different contexts. In a previous work,[11] we showed that DFT provides accurate descriptions of the characteristics of nanoparticle and diblock copolymer mixtures under confinement. The DFT was used to investigate the distribution of nanoparticles in the dilute limit.[12] The purpose of the present work is to investigate the morphology and elasticity of diblock-copolymer composites at finite concentration of nanoparticles. We make further comparisons of the theoretical predictions with simulation data for the lamellar structures of block-copolymer melts and with recent experiments on the distribution of nanoparticles in the copolymer structure. In addition, we investigate, for the first time with DFT, the effect of nanoparticles on the elastic properties of an ordered nanocomposite in the lamellar phase, over a range of particle properties.

The remainder of this article is organized as follows. After a brief description of the molecular model and theoretical methods, we discuss the DFT predictions of the effects of nanoparticles on the lamellar structure and periodic spacing over a broad range of molecular and thermodynamic parameters. We investigate particle dispersion in both symmetric and asymmetric block copolymer structures. When appropriate, the theoretical predictions are compared with results from molecular dynamics simulations. Next, we examine the elastic properties of the composite in terms of the extension/compression moduli. We compare the theoretical results for the effects of particle size and concentration on the elasticity of the copolymer with macroscopic experimental observations, the SCFT predictions and Monte Carlo simulations.

2. Molecular Model and Theoretical Background

As discussed in previous works,[12,13] we assume that nanoparticles can be represented by structureless spheres and diblock copolymers are represented by tangentially connected chains of spherical segments. Each diblock copolymer chain consists of two types of segments, designated as "A" and "B", with the same size (diameter σ_s) but different interaction energies. The average packing fraction ($\pi\rho_{AV}\sigma_S^3/6$, where ρ_{AV} is the average monomer density) of the polymer segments is larger than 0.3, close to that of a polymer melt. For comparison with the simulation results, we use relatively short chains ($N = 20$ segments per chain) but longer chains will be used for predicting the microphases of copolymer−nanoparticle composites ($N = 100$) and for investigating the elastic properties of the composites ($N = 50$ or 100).

The pair interaction between copolymer segments and nanoparticles is described by a square-well (SW) potential[11]

$$\varphi_{ij}(r) = \begin{cases} \infty & r < \sigma_{ij} \\ -\varepsilon_{ij} & \sigma_{ij} \le r \le \gamma\sigma_{ij} \\ 0 & r > \gamma\sigma_{ij} \end{cases} \quad (1)$$

where subscripts i and j denote a polymer segment or a nanoparticle, ε_{ij} represents the strength of the pair interaction energy, $\sigma_{ij} = (\sigma_i + \sigma_j)/2$, and γ specifies the range of attraction (or repulsion). Throughout this work, the parameters related to nanoparticles are labeled with subscript "P", and those affiliated with a polymer segment are labeled with subscript "S". For comparison with simulation results, we assume that A and B segments repel each other with a square-shoulder potential of strength ε_{AB} that extends to $2\sigma_S$; the nanoparticles are neutral to B segments but repel A segments with strength ε_{AP} and the range of repulsion is set at $\sigma_S = (\sigma_P + \sigma_S)/2$. Unless specifically indicated, we assume $\gamma = 2$ for all other cases. The polymer segments of the same type interact strictly with the excluded volume interactions (i.e., $\varepsilon_{AA} = \varepsilon_{BB} = 0$), and a "square-shoulder" repulsion is imposed between different polymer segments ($\varepsilon_{AB} < 0$) to facilitate the microphase segregation of copolymer segments. In addition to the excluded-volume effect, the interaction between a particle and a polymer segment can be either repulsive or attractive. Dimensionless units are used for both energy and length parameters, e.g., $\varepsilon^* = \varepsilon/k_BT$ and $\sigma_P^* = \sigma_P/\sigma_S$, with k_B being the Boltzmann constant and T the absolute temperature.

The DFT calculations are based on a free-energy functional applicable to particle−diblock copolymer mixtures within a self-consistent theoretical framework.[11] Briefly, the Helmholtz free energy functional includes an expression for the ideal chains that preserves the bond potential and the molecular topology, and an excess term arising from nonbonded intra- and inter- molecular interactions

$$\beta F_{ex}[\{\rho_j(\mathbf{r})\}] = \int d\mathbf{r}\, \{\phi^{hs}[n_\alpha(\mathbf{r})] + \phi^{chain}[n_\alpha(\mathbf{r})]\} + \beta F_{ex}^{att}[\{\rho_j(\mathbf{r})\}] \quad (2)$$

where $\beta = 1/k_BT$. In eq 2, $\rho_j(\mathbf{r})$, is the density profile of species j; ϕ^{hs} and ϕ^{chain} are the Helmholtz energy densities due to the excluded-volume effects and the intrachain correlations, respectively; $n_\alpha(\mathbf{r})$, $\alpha = 0, 1, 2, V1, V2$, are weighted densities, and F_{ex}^{att} represents the Helmholtz energy functional due to the square-well interactions beyond the hard-sphere collision. We refer to previous publications for detailed expressions of the different terms on the right side of eq 2.[14,15]

At equilibrium, the density profiles of polymer segments and nanoparticles are calculated by solving the Euler−Lagrange equations, obtained by minimization of the grand potential.[11] For a polymer−nanoparticle system with a lamellar structure, the density profiles vary only in the direction perpendicular to the lamellar interface. In that case, the density profiles are calculated from

$$\rho_A(z) = \rho_{AV}D \times \frac{\sum_{i=1}^{N_A} G_L^i(z)\exp[-\beta\lambda_i(z)]G_R^i(z)}{\int \sum_{i=1}^{N_A} G_L^i(z)\exp[-\beta\lambda_i(z)]G_R^i(z)\,dz} \times \frac{N_A}{N} \quad (3)$$

$$\rho_B(z) = \rho_{AV}D \times \frac{\sum_{i=N_A+1}^{N_A+N_B} G_L^i(z)\exp[-\beta\lambda_i(z)]\cdot G_R^i(z)}{\int \sum_{i=N_A+1}^{N_A+N_B} G_L^i(z)\exp[-\beta\lambda_i(z)]\cdot G_R^i(z)\,dz} \times \frac{N_B}{N} \quad (4)$$

$$\rho_p(z) = \rho_{AVP} D \times \frac{\exp[-\frac{\delta\beta F_{ex}}{\delta\rho_p(z)}]}{\int \exp[-\frac{\delta\beta F_{ex}}{\delta\rho_p(z)}]\, dz} \quad (5)$$

In eqs 3−5, z represents the direction perpendicular to the lamellae, D is the lamellar thickness, ρ_{AV} and ρ_{AVP} are the average densities of the polymer segments and nanoparticles, N is the total degree of polymerization for the diblock copolymer, and N_A and N_B are the numbers of segments in the A and B blocks per chain, respectively. The recurrence functions $G^i_L(z)$ and $G^i_R(z)$ are calculated from

$$G^i_L(z) = \frac{1}{2\sigma_s}\int_{z-\sigma_s}^{z+\sigma_s} \exp[-\beta\lambda_{i-1}(z)] G^{i-1}_L(z)\, dz \quad (6)$$

$$G^i_R(z) = \frac{1}{2\sigma_s}\int_{z-\sigma_s}^{z+\sigma_s} \exp[-\beta\lambda_{i+1}(z)] G^{i+1}_R(z)\, dz \quad (7)$$

with the initial values $G^1_L(z)=1$ and $G^N_R(z)=1$.[14] The self-consistent fields $\lambda_i(z)$ are related to the excess Helmholtz energy functional F_{ex} by

$$\lambda_A(z) = \frac{\delta F_{ex}}{\delta\rho_A(z)} \quad (8)$$

$$\lambda_B(z) = \frac{\delta F_{ex}}{\delta\rho_B(z)} \quad (9)$$

While the one-dimensional density profiles provide no information on the composite structure in the directions parallel to the lamellar layers, the correlations in these directions are partially accounted for through the formulation of the excess Helmholtz energy functional. In other words, the excess Helmholtz energy functional reduces to a non-mean-field equation of state even when the density is uniform.

In calculating the microstructure of a copolymer composite, we fix the average densities of the diblock copolymers and nanoparticles, and apply a periodic boundary condition to the direction perpendicular to the lamellar interface (z-direction). Given the block polymer backbone structure and the average densities for the polymer segments (designated as ρ_{AV}) and for the particles (designated as ρ_{AVP}), eqs 3−9 are solved simultaneously for the density profiles by using the Picard iteration method. The periodic lamellar spacing D is determined by minimization of the Helmholtz free energy, which can be calculated from eq 2 with the polymer and particle density profiles as the input.

When the composite undergoes an extension or compression in the direction perpendicular to the lamellae, the relative deformation is described by $\delta = d/L$, where d is the absolute extension or compression, and L is the length of the material in the direction of deformation before extension or compression. The composite is in a constrained equilibrium state after extension or compression, where the number of lamellae does not change. On the basis of the standard theory of linear elasticity,[10] the elastic free energy can be written as

$$F_{el} = 1/2 K_{33}\delta^2 \quad (10)$$

where F_{el} is the Helmholtz free energy of the composite under deformation, and K_{33} is obtained from the second derivative $\partial^2 F_{el}/\delta\partial^2$. From the extensional modulus K_{33} and shear modulus K_{44}, we can calculate the tensile (Young's) modulus

$$E = \frac{K_{33}(K_{33}+6K_{44})}{12(K_{33}+K_{44})} \quad (11)$$

Because the nanoparticle-block polymer mixture is in a liquid state (melt), K_{44} is sufficiently small so that it can be ignored in calculations of the tensile modulus E.[16] In this case, tensile modulus E is directly proportional to extensional modulus K_{33}.

3. Results and Discussion

3.1. Composite Microstructure. The dispersion of nanoparticles in a lamellar structure depends on the particle volume fraction, surface energy and the ratio of the particle diameter σ_P and the lamellar periodicity D. In general, large particles are difficult to be homogeneously dispersed in a block copolymer melt, but rather aggregate and separate into macroscopic phases.[7] To identify systems free of the macroscopic segregation, we compare the Helmholtz free energy of the composites in macrophase separation and that in microphase separation to ensure that for a given set of parameters the lamellar state has a lower free energy. For all systems considered in this work, we verified that the lamellar structure is thermodynamically stable; i.e., it is free of macroscopic segregation. We found that the system would result in a macroscopic segregation only if the repulsive strength of the pair interaction between A and B segments is below a certain value. This critical repulsive strength depends on the packing fraction of the particles. The conditions that we choose for the lamellar structures are far above this critical value.

We first compare the density profiles of nanoparticles and polymer segments in nanocomposites of symmetric diblock copolymer with those reported by molecular dynamics simulations.[17] Figure 1 shows typical reduced density profiles of A and B segments and of the nanoparticles with different sizes and surface energies within one lamellar periodic spacing. The parameters used in our DFT calculations are the same as those of Figure 4 in the molecular dynamics simulations.[17] Throughout this work, the reduced density is defined as the local density divided by the average density of the corresponding species.

Parts a, d, and g of Figure 1 show the density profiles for polymer segments and neutral particles. As shown in molecular dynamics simulations, the nanoparticles are preferentially localized at the copolymer interface, leading to a decrease of the lamellar interfacial tension.[18] The nanoparticles have a stronger tendency to localize at the lamellar interface as the particle size is increased. While the density profiles of the nanoparticles are sensitive to their size, relatively little change is observed in the density profiles of the lamellar structure, except that the interface becomes slightly less distinctive as the particle size is increased. As shown by simulations, the theoretical results indicate that the nanoparticles not only fill the voids at the lamellar interface, but also affect the interfacial structure.

Parts b, e and h of Figure 1 show the density profiles for particles that are energetically biased to a particular block copolymer domain ($\varepsilon^*_{AP}/\varepsilon^*_{AB}=1$). We find that nanoparticles with moderate repulsion to the A segments have stronger influence on the copolymer structure than neutral nanoparticles. While small particles ($\sigma^*_P = 1$) exhibit a preference for the center of the B domains, larger particles ($\sigma^*_P = 4$) prefer the lamellar interface. Particles of intermediate size ($\sigma^*_P = 2$) are found in both locations, with a slightly stronger preference near the interface. The variation of the particle distribution with size reflects a competition between the interfacial tension and energetic affinity. As found in the simulation,[17] at high particle density, the density profiles of copolymer segments become more sensitive to the particle size. For particles of small and moderate sizes ($\sigma^*_P = 1$ and 2),

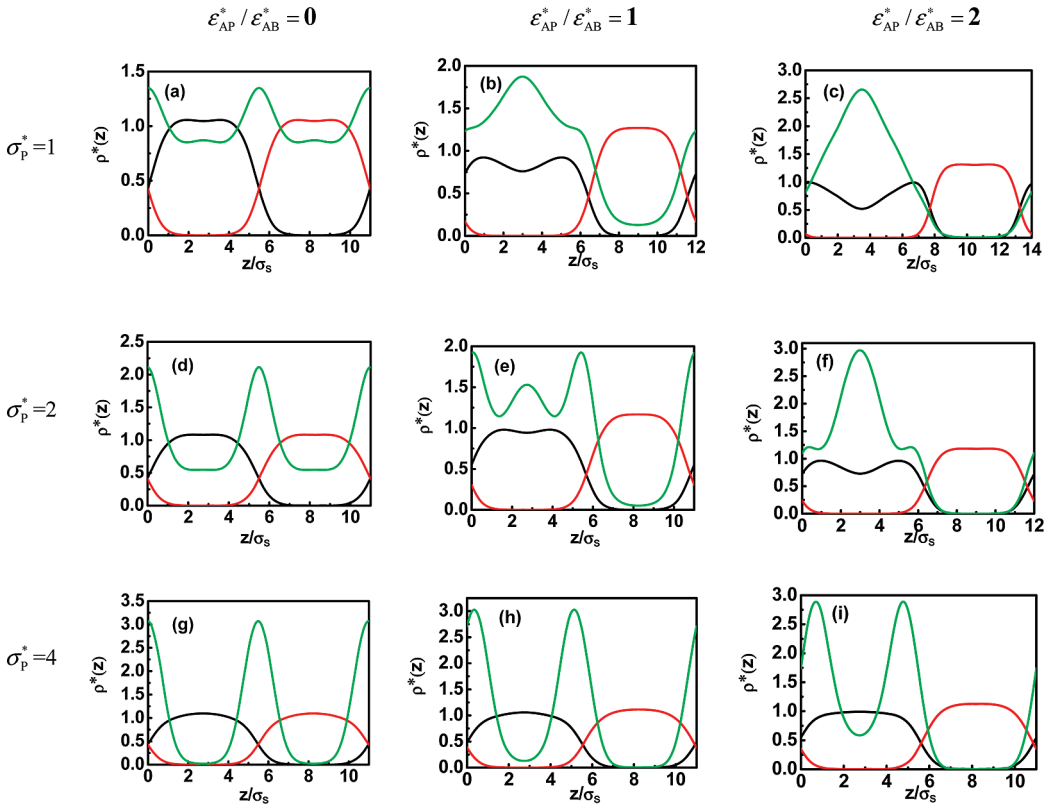

Figure 1. (a) Density profiles of the polymer segments ("A" and "B") and nanoparticles ("P") within a lamellar period of a symmetric diblock copolymer. Here the relative diameter of the particles is $\sigma^*_P = 1$, 2, and 4 (rows 1, 2 and 3) and the relative interaction energy between the particle and "A" segment is $\varepsilon^*_{AP}/\varepsilon^*_{AB} = 0$, 1, and 2 (columns 1, 2 and 3). In all cases, the interaction energies among the polymer segments are $\varepsilon^*_{AA} = \varepsilon^*_{BB} = 0$, $\varepsilon^*_{AB} = -0.125$, the polymer chain length is $N = 20$, the average packing fraction of the polymer is 0.28 and that for the particles is 0.07. In all plots, domain B is on the left and A is on the right.

the polymer density in the B domain center is significantly depressed due to the excluded volume of the dissolved nanoparticles.

As the biased energy further increases ($\varepsilon^*_{AP}/\varepsilon^*_{AB} = 2$ in Figure 1, parts c, f, and i), the nanoparticles have a stronger preference for domain B. Consistent with the simulation results,[17] the particles of $\sigma^*_P = 2$ are more localized in domain B than those of $\sigma^*_P = 1$. The dependence of the particle density profile on size (for $\sigma^*_P = 1$ and 2) is different from that when the particle has moderate repulsion with A ($\varepsilon^*_{AP}/\varepsilon^*_{AB} = 1$). A comparison of Figure 1h and Figure 1i ($\sigma^*_P = 4$) indicates that with the repulsion between the particle and A segments, the peaks of the particle density profiles are totally confined within the B domain. While for small particles the DFT predictions are in good agreement with the simulation results, the multiple peaks in the concentration profiles of large nanoparticle ($\sigma^*_P = 4$) were not shown in the simulation. The discrepancy can be attributed to the fact that the DFT gives a slightly higher concentration of nanoparticles in the resident polymer domain. In comparison to the simulation, the DFT overpredicts the degree of microphase separation in the diblock copolymer.

In addition to the particle size and energy, the polymer architecture plays an important role in determining the microstructure of the copolymer/nanoparticle composites. As an example, Figure 2 shows the distribution of nanoparticles within an asymmetric copolymer in which each chain contains $N_A = 35$ A segments and $N_B = 65$ B segments. As for the symmetric case, the system organizes into a lamellar structure, and the repulsion between the particles and the B block leads the particles to preferentially localize in the A domain. Figure 2a shows that at high particle density, the

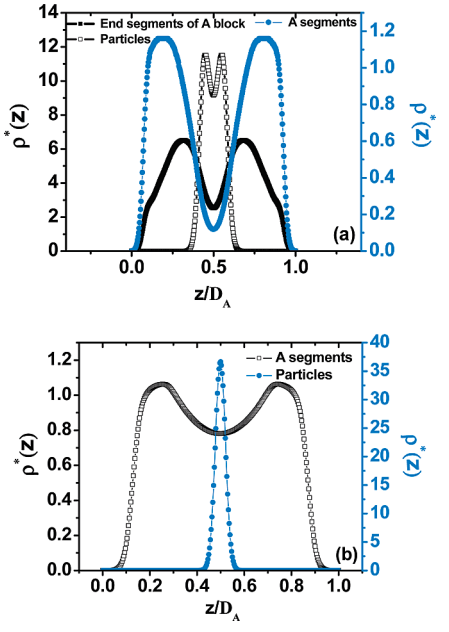

Figure 2. Effect of the particle concentration on the density profiles of "A" segments and nanoparticles (note that only the A domain is shown). The particle packing fraction is 0.1 in (a) and 0.03 in (b). In both cases, the polymer packing fraction is 0.32; the particle and polymer interaction energies are $\varepsilon^*_{AB} = \varepsilon^*_{BP} = -0.2$, $\varepsilon^*_{AA} = \varepsilon^*_{BB} = 0$, $\varepsilon^*_{AB} = -0.125$; the particle diameter is $\sigma^*_P = 6$, the polymer chain length is $N = 100$; and the number of "A" segments in each polymer chain is $N_A = 35$. D_A is the thickness of the A domain.

DFT predicts double peaks of the particle density profile in the A domain, suggesting that the particles reside at the ends

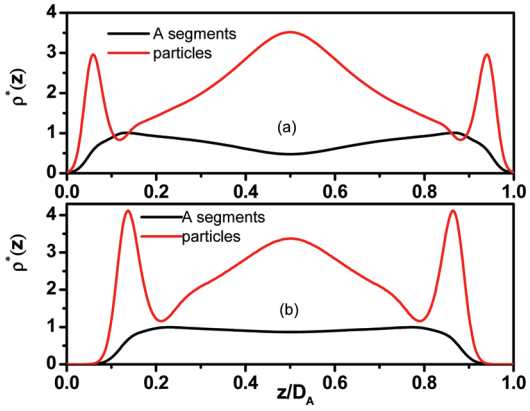

Figure 3. Same as Figure 2 but for smaller particles ($\sigma_P^* = 2$).

of the chains within the A block. Conversely, at low particle volume fraction, the particles are concentrated at the domain center, as shown in Figure 2b. In this case, the A blocks are much less stretched (as indicated by the size of the A domain). Qualitatively, the density profiles shown in Figure 2 are in good agreement with SCFT predictions on a similar system by Thompson et al.[6] In particular, both calculations predict two peaks in the particle density for larger particle volume fractions and one peak in the density at smaller particle volume fractions.

Figure 3 shows the predictions from DFT for the same system as in Figure 2 but with smaller nanoparticles. When the particle volume fraction is small, the particle distribution in the A block (Figure 3b) resembles that in the B block shown in Figure 1e, i.e., particles with moderate size and moderate energy affinity have two different preferential locations. Integration of the particle density under the peaks shows that about 29% of the particles are located at the interfaces. At higher particle volume fraction (Figure 3a), however, only about 15% of the particles are located at the interfaces, with the rest favoring the domain center. The drastic decrease of the fraction of particles at the interface is likely due to the particles becoming saturated at the interface so that as their concentration increases they are more likely to be found in the domain center.

In previous work,[12,13] we investigated the distribution of nanoparticles in a symmetric diblock copolymer system with $\varepsilon_{AA}^* = \varepsilon_{BB}^* = 0$ and nanoparticles energetically biased toward a specific domain of the lamellae. We found that particles energetically favorable with just one block tend to localize at the center of their preferred microdomain. At finite concentration, the distribution of nanoparticles is also affected by the interaction between nanoparticles in addition to their size and surface energy. Besides, the exact location of particles is sensitive to interactions among polymer segments. Figure 4 shows the effects of introducing an attraction between the same polymer segments on the particle distribution. In this case, particles preferring microdomain A are mostly located at the interface. As the particle size decreases from $\sigma_P^* = 7$ to $\sigma_P^* = 1$, particles move from the interface toward being uniform throughout both domains. Thus introducing an attraction between the same polymer segments, in addition to the particle surface energy, may provide a new route to control nanoparticle distributions.

To summarize the DFT results on the microstructure of copolymer composites, we find that neutral nanoparticles tend to localize near the interfaces in lamellar diblock copolymers. The locations of energetically selective particles depend on their size, density, and whether there are also attractive interactions between the same polymer segments.

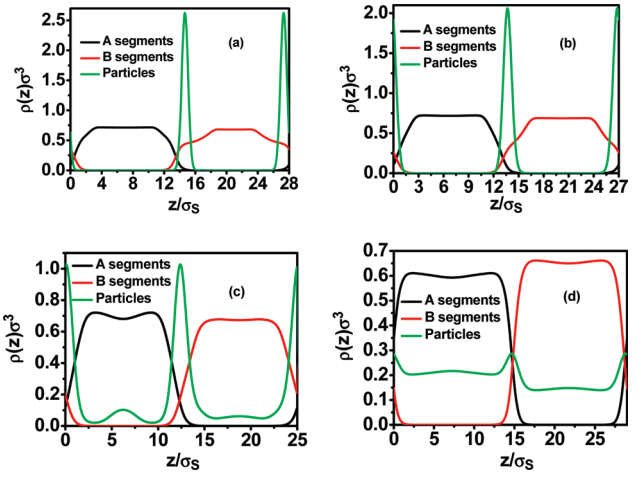

Figure 4. Density profiles of the polymeric segments ("A" and "B") and nanoparticles for $\varepsilon_{AB}^* = -0.05$, $\varepsilon_{AA}^* = \varepsilon_{AB}^* = 0.05$ within a lamellar period of a symmetric diblock copolymer. Particle size is $\sigma_P^* = 7$ (a), $\sigma_P^* = 5$ (b), $\sigma_P^* = 3$ (c), and $\sigma_P^* = 1$ (d). Packing fraction for the polymer is 0.32, and that for the particles is 0.05. The polymer chain length is $N = 100$.

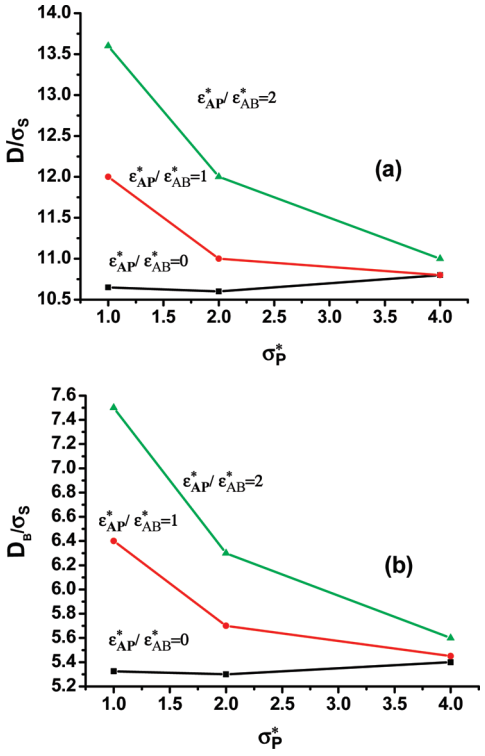

Figure 5. (a) Effect of the particle size and particle−polymer interaction energy on the lamellar spacing D. (b) Effect of nanoparticle diameter and energy on the dimension of a neutral domain ("B") D_B. The polymer parameters are the same as those in Figure 1.

3.2. Lamellar Structure and Periodic Spacing. Figure 5a shows the lamellar spacing for the same systems as in Figure 1 in response to the changes in the particle sizes and energy parameters. For all cases, the lamellar spacing without the particles is $D = 10.9\sigma_S$. In agreement with experiments,[22] we find that small neutral particles reduce the periodic spacing and that energetically selective particles swell the periodic spacing. In particular, particles with higher energy preference cause a larger expansion of the lamellar thickness. As shown in Figure 5b, the thickness of the B domain, i.e., the domain that is neutral to the nanoparticles, varies in accordance with that of the overall lamellar spacing, indicating

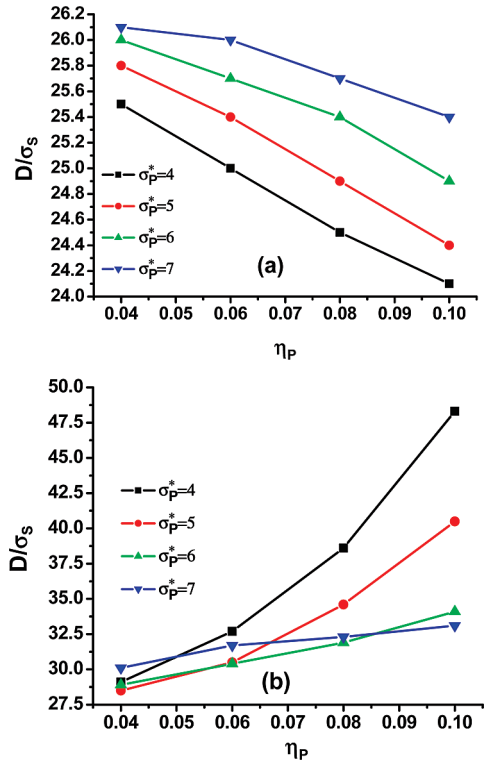

Figure 6. Effect of particle packing fraction on the lamellar spacing of a symmetric diblock copolymer. (a) Neutral particles with diameter $\sigma_P^* = 4, 5, 6$ and 7. (b) Particles biased toward "A" domain ($\varepsilon_{AP}^* = 0.5$). In both cases, $\varepsilon_{AA}^* = \varepsilon_{BB}^* = 0$, $\varepsilon_{AB}^* = -0.05$. The polymer chain length is $N = 100$.

that the changes of the energetically favorable domain size are mainly responsible for the lamellar swelling. Note that for energetically selective particles, the particles move from the center of the B domain toward the interfaces as the size increases (see Figure 1), resulting in less swelling and a decrease of the overall lamellar thickness.

Parts a and b of Figure 6 show the variation of the lamellar spacing as a function of the particle packing fraction for neutral and energetically selective particles respectively. For neutral particles (Figure 6a), the lamellae are more compressed as the particle packing density is increased. The reduction of lamellar thickness arises from the decrease in the AB interfacial tension due to the positioning of the particles at the interface. In that case, the polymer chains become less stretched because they have fewer unfavorable AB contacts. The theoretical results are consistent with experiments by Kim et al.[19] It was observed that increasing volume fractions of neutral Au nanoparticles, designated to segregate to the interfaces of the lamellar diblock copolymer PS-*b*-P2VP, causes a decrease in the lamellar period. Figure 6b shows the swelling of the lamellar thickness when the volume fraction of selective particles is increased. For particles that are energetically biased to a specific (B) domain, the swelling of the lamellae can be attributed to the increased particle packing density within the polymer matrix. Centralization of the particles at the compatible domain center excludes polymer segments and thereby increases the lamellar thickness. The magnitude of the swelling becomes smaller as the particle size is increased from $\sigma_P^* = 4$ to $\sigma_P^* = 7$ due to the decrease of the polymer sensitivity to the particles as the size increases. In general, the degree of swelling or contraction is dependent on the size of the particles and their volume fraction. The magnitude of the shrinkage or swelling predicted by DFT is in qualitative agreement with a strong segregation theory recently proposed by Pryamitsyn and Ganesan.[18]

3.3. Extensional Moduli of Copolymer Nanocomposite Materials. Introduction of nanoparticles into a polymer matrix affects not only the microscopic structure but also its mechanical properties. For simplicity, here we focus only on composites composed of symmetric diblock copolymers and nanoparticles. There is no interaction, other than the excluded volume effect, between polymer segments of the same type. The formation of the lamellar structure is solely due to the repulsion between segments in A and B blocks. We are interested in the effects of particle volume fraction and size on the moduli of neutral-particle-filled copolymer systems. In addition, we investigate how the extensional modulus is influenced by the particle-polymer interactions.

In the bulk state, the lamellar spacing will be increased or decreased under constrained equilibrium, i.e., when the composite is extended or compressed in the direction perpendicular to the interface. As a result, the distribution of the nanoparticles is also changed, which corresponds to a compression or expansion of the lamellae, resulting in a smaller or larger packing density of the composite.[20] As discussed earlier, the extensional modulus of a copolymer/nanoparticle composite can be calculated from a linear elasticity theory (eq 10). A small extension or compression of the lamellar system leads to a free-energy change related to the mechanical modulus. In this work, we extend or compress the lamellae in the direction perpendicular to the interface by a small deformation δ and calculate the free energy at each deformation. The curves of total free energies versus the relative distortion show parabolic shapes, indicating that the linear elasticity theory is appropriate. The free-energy curves are then fitted with polynomials and the second derivatives are used to calculate K_{33}.[16]

We find that large neutral nanoparticles behave as reinforcing agents, while smaller neutral particles often behave as plasticizers, in agreement with experiments.[21] The particle size plays an important role in contributing to the mechanical properties of a composite material.[22] While addition of nanofillers usually strengthens a homopolymer nanocomposite, our DFT calculations suggest that small neutral particles do not increase the extensional modulus of a block copolymer composite. For example, a composite composed of symmetric diblock copolymers ($N = 100$, packing fraction of 0.32, $\varepsilon_{AB} = -0.05$) and neutral nanoparticles ($\sigma_P^* = 3$, packing fraction of 0.05) has the same dimensionless extensional modulus K_{33} as the pure diblock ($\beta K_{33} = 0.0751$). A decrease of the extensional modulus ($\beta K_{33} = 0.06378$) is predicted when the particle packing fraction is increased to 0.1. The decrease of the extensional modulus suggests that small neutral particles serve as plasticizers in a block copolymer composite. On the contrary, the theoretical calculations indicate that large neutral particles may lead to a moderate increase of the extensional modulus. For example, addition of particles of $\sigma_P^* = 7$ and particle packing fraction of 0.05 enhances the extensional modulus of the same block copolymer by 8.9%.

In contrast to neutral particles, the DFT calculations indicate that small but energetically selective particles can serve as reinforcing agents of the composite material. Table 1 shows the extensional moduli of the composite materials with particles of $\sigma_P^* = 3$ as the fillers under four combinations of energetic parameters. We find that particles attractive to one block but repulsive to the other block work the best to reinforce the mechanical strength of the materials. Table 2 shows K_{33} at different energy parameters for a composite

Table 1. Elastics Modulus (K_{33}, in Units of k_BT) for a Symmetric Diblock Copolymer Filled with 5% Nanoparticles at Different Particle−Polymer Energetic Parameters[a]

interaction energy	$\varepsilon^*_{BP}=0$ and $\varepsilon^*_{AP}=0.1$	$\varepsilon^*_{AB}=-\varepsilon^*_{BP}=0.05$	$\varepsilon^*_{AP}=-2\varepsilon^*_{BP}=0.1$	$\varepsilon^*_{AP}=-\varepsilon^*_{BP}=0.1$
K_{33}	0.08232 (9.96%)	0.08330 (10.9%)	0.09190 (22.3%)	0.09610 (27.96%)

[a] In all cases, $\varepsilon^*_{AB}=-0.05$, $\sigma^*_P=3$, and $N=100$. The parentheses give the percentage increase of the elastic modulus in comparison with that of the pure copolymer.

Table 2. Elastics Modulus for Composites Containing 5% Nanoparticles with $\sigma^*_P=5$[a]

interaction energy	$\varepsilon^*_{AP}=-\varepsilon^*_{AB}=0.05$; $\varepsilon^*_{BP}=0$	$\varepsilon^*_{AP}=-2\varepsilon^*_{AB}=0.1$; $\varepsilon^*_{BP}=0$	$\varepsilon^*_{AP}=-\varepsilon^*_{AB}=0.05$; $\varepsilon^*_{BP}=-0.05$
K_{33}	0.08566 (14%)	0.11016 (46.68%)	0.11552 (53.82%)

[a] All other parameters are the same as those appearing in Table 1.

filled with $\sigma^*_P = 5$ particles. Our theoretical calculations suggest that energetically selective particles are more efficient than neutral particles to increase the elastic modulus of the block copolymer.

The filler volume fraction plays an important role in the material reinforcement.[21] For example, the pure diblock system composed of 50 segments ($\varepsilon^*_{AB} = -0.05$) has an extensional modulus $\beta K_{33} = 0.09994$. When the same block copolymer system is filled with neutral particles of moderate size ($\sigma^*_P=5$) at $\eta_p=0.1$, the extensional modulus K_{33} increases by 23.07%. One may expect that addition of more neutral nanofillers would further strengthen the composite. However, doubling the volume fraction of the neutral particles ($\eta_P=0.2$) results in only marginal changes in K_{33}, which increases only by an additional 2.28% in comparison to the value at $\eta_p=0.1$. The increase of the extensional modulus of the composite material is probably due to the shrinkage of the lamellar domain when the packing fraction of neutral particles is increased. The external modulus reaches a plateau beyond a certain particle density.

In the only previous theoretical calculations of elastic modulus for diblock nanocomposites, Thompson et al.[10] found that small, energetically selective particles lead to a decrease in the modulus. However, they only studied one system in that work, and used a hybrid SCFT/DFT theory as opposed to the DFT used here which treats all species with the same theory.

Our DFT calculations suggest that neutral nanoparticles can increase or decrease the elastic modulus of a composite material, depending on the particle size, surface energy and concentration. In general, large nanoparticles reinforce the extensional moduli of copolymers; the effects of small particles are sensitive to their sizes and interactions. Simulations and experiments support that filler particles cause an extension or contraction of the chains, thereby changing the stress required for elastic deformation.[23,24] The reinforcement effect of attractive and large neutral particles is in good agreement with the notion that the elastic modulus can increase to a larger extent when particles agglomerate than when they are evenly dispersed. Unlike small neutral particles, large energetically selective particles tend to aggregate within the lamellar structure, leading to enhanced mechanical properties.

4. Conclusions

This work represents the first application of the density functional theory to polymer−nanoparticle composites at a wide variety of system parameters. It predicts the effects of particle size, surface energy and packing density on lamellar structure in good qualitative agreement with simulation results and experiments. The work is significant because a comprehensive theory for polymer−particle systems is yet to be established.

Introduction of an energetic preference for one block leads to accumulation of particles into a particular microdomain. Particles with intermediate size may form a layered structure within the energetically biased microdomain. These results are shown to match with simulation results and experiments qualitatively. Besides the particle size, the packing fraction of nanoparticles plays an essential role in controlling the final structure of the copolymer nanocomposites. Large packing fraction results in particle centralization at the desired locations regardless of the particle size. In this case, the particle size only affects the local microstructure of the composites. For selective particles, a robust way to control their location is by adding interactive energy among the segments of the same type. Concerning the role of nanoparticles in influencing the lamellar spacing, we find that neutral particles tend to localize at the interface, which leads to a contraction of the lamellae, while selective particles segregate into their preferred phase and swell the lamellar domain. Whereas the periodic spacing is sensitive to the concentration of small nanoparticles, the theory predicts diminishing effects for large nanoparticles at the same volume fraction.

By using the DFT, we clarified that small nanoparticles can either increase or decrease the extensional moduli of a composite material, depending on the cooperative effects of their size, volume fraction and interactions. Conversely, large particles reinforce copolymers regardless of copolymer−particle interaction. By variation of the polymer−nanoparticle interaction, we may identify important parameters for the design of nanocomposite systems with desired mechanical properties.

Acknowledgment. This research is sponsored by the U.S. Department of Energy (DE-FG02-06ER46296) and uses the computational resources from the National Energy Research Scientific Computing Center (NERSC), which is supported by the Office of Science of the U.S. Department of Energy under Contract No. DE-AC03-76SF0009. This work was also performed in part at the US Department of Energy, Center for Integrated Nanotechnologies, at Los Alamos National Laboratory (Contract DE-AC52-06NA25396) and Sandia National Laboratories (Contract DE-AC04-94AL85000)

References and Notes

(1) Bockstaller, M. R.; Mickiewicz, R. A.; Thomas, E. L. *Adv. Mater.* **2005**, *17*, 1331.
(2) Balazs, A. C. *Annu. Rev. Phys. Chem.* **2007**, *58*, 211.
(3) Balazs, A. C.; Emrick, T.; Russell, T. P. *Science* **2006**, *314* (5802), 1107.
(4) Bockstaller, M. R.; Thomas, E. L. *Phys. Rev. Lett.* **2004**, *93*, 166106.
(5) Liff, S. M.; Kumar, N.; McKinley, G. H. *Nat. Mater.* **2007**, *6* (1), 76. Manias, E. *Nat. Mater.* **2007**, *6* (1), 9.
(6) Thompson, R. B.; Ginzburg, V. V.; Matsen, M. W.; Balazs, A. C. *Science* **2001**, *292* (5526), 2469.
(7) Kim, B. J.; Chiu, J. J.; Bang, L.; Hawker, C. J.; Pine, D. J.; Kramer, E. J. *Abstr. Pap., Am. Chem. Soc.* **2005**, *230*, U1066. Kim, J. U.; O'Shaughnessy, B. *Macromolecules* **2006**, *39*, 413. Kim, B. J.; Given-Beck, S.; Bang, J.; HawkerO, C. J.; Kramer, E. J. *Macromolecules* **2007**, *40*, 1796.
(8) Tyler, C. A.; Morse, D. C. *Macromolecules* **2003**, *36*, 3764.

(9) Kossuth, M. B.; Morse, D. C.; Bates, F. S. *J. Rheol.* **1999**, *43* (1), 167.
(10) Thompson, R. B.; Rasmussen, K. O.; Lookman, T. *Nano Lett.* **2004**, *4*, 2455.
(11) Cao, D. P.; Wu, J. Z. *J. Chem. Phys.* **2007**, *126*, 144912.
(12) Jin, J. Z.; Wu, J. Z. *J. Chem. Phys.* **2008**, *128*, 032803.
(13) Cao, D. P.; Wu, J. Z. *Macromolecules* **2005**, *38*, 971.
(14) Yu, Y. X.; Wu, J. Z. *J. Chem. Phys.* **2002**, *117*, 10156.
(15) Li, Z. D.; Cao, D. P.; Wu, J. Z. *J. Chem. Phys.* **2005**, *122*, 174708.
(16) Thompson, R. B.; Rasmussen, K. O.; Lookman, T. *J. Chem. Phys.* **2004**, *120*, 3990.
(17) Schultz, A. J.; Hall, C. K.; Genzer, J. *Macromolecules* **2005**, *38*, 3007.
(18) Pryamitsyn, V.; Ganesan, V. *Macromolecules* **2006**, *39*, 8499.
(19) Kim, B. J.; Fredrickson, G. H.; Hawker, C. J.; Kramer, E. J. *Langmuir* **2007**, *23*, 7804.
(20) Kang, H. M.; Detcheverry, F. A.; Mangham, A. N.; Stoykovich, M. P.; Daoulas, K. C.; Hamers, R. J.; Muller, M.; de Pablo, J. J.; Nealy, P. F. *Phys. Rev. Lett.* **2008**, *100*, 148303.
(21) Papakonstantopoulos, G. J.; Doxastakis, M.; Nealey, P. F.; Barrat, J. L.; de Pablo, J. J. *Phys. Rev. E* **2007**, *75*, 031803.
(22) Yang, K.; Yang, Q.; Li, G. X.; Sun, Y. J.; Feng, D. C. *Polym. Compos.* **2006**, *27*, 443. Dikobe, D. G.; Luyt, A. S. *J. Appl. Polym. Sci.* **2007**, *103*, 3645.
(23) Doxastakis, M.; Chen, Y.-L.; Guzman, O.; Pablo, J. J. d. *J. Chem. Phys.* **2004**, *120*, 9335. Nakatani, A. I.; Chen, W.; Schmidt, R. G.; Gordon, G. V.; Han, C. C. *Polymer* **2001**, *42*, 3713.
(24) Tuteja, A.; Duxbury, P. M.; Mackay, M. E. *Phys. Rev. Lett.* **2008**, *100*, 077801.